



Preparation and characterization of PEG/PVDF composite membranes and effects of solvents on its pervaporation performance in heptane desulfurization

Zhengjin Yang, Weiyu Zhang, Jiding Li*, Jian Chen

Department of Chemical Engineering, State Key Laboratory of Chemical Engineering, Tsinghua University, Beijing 100084, China

Tel. +86 10 62773234; Fax: +86 10 62782432; email: lijiding@mail.tsinghua.edu.cn

Received 24 November 2011; Accepted 5 February 2012

ABSTRACT

Polyethylene glycol/polyvinylidene fluoride (PEG/PVDF) composite membranes were prepared using different water–organic solvent mixtures and the composite membranes obtained were characterized by Fourier transform infrared spectroscopy (FTIR-ATR), scanning electron microscopy, wide-angle X-ray diffraction (WAXD), and X photoelectron spectroscopy (XPS). Pervaporation (PV) experiments were conducted to characterize the sulfur removal properties of the PEG/PVDF composite membranes using a feed mixture of heptane and ethyl thioether with a sulfur concentration of 300 ng/ μ L over the temperature range of 65–80°C. All membranes investigated in this work showed proper PV performance and the E-PEG exhibited the highest PV flux and the highest sulfur enrichment factor of 5.17 at 65°C. The correlation of membrane crystallinity and surface oxygen content with PV performance was established. A decrease in membrane crystallinity or an increase in surface oxygen content greatly improved the membrane desulfurization property which was due to a decrease in mass transport resistance and an increase in sorption at membrane surface respectively. Finally, suggestions on the establishment of mass transfer model in PV process were made based on the results of the WAXD, FTIR-ATR, XPS studies and PV experiments.

Keywords: Composite membrane; Pervaporation; Desulfurization; Solvent effect

1. Introduction

Gasoline has been the most important energy supplier in the past five decades. However, contaminants released in the consumption of gasoline make up the biggest part of air pollution. For example, the burning of sulfur impurities directly contributes to the emission of SO_x. Nowadays, pollution caused by gasoline combustion has aroused worldwide environmental concerns. With the increasing requirement for cleaner

air, governments all around the world are working together to make stringent clean air regulation, especially the sulfur content limitation in the gasoline products [1,2]. A number of sulfur removal techniques, such as hydro-treating [3], adsorption [4], and extraction [5], are proposed. However, none of them has proved to be of industrial perfection. Thus, there is an urgent need to explore a more efficient method for gasoline desulfurization. Pervaporation (PV) is a promising candidate in this direction. In the PV process, the feed mixture is circulated at the upside of the membrane and the preferentially permeated

*Corresponding author.

component is enriched and collected at the low pressure downside of the membrane. The low pressure is obtained normally by using a cold trap, a vacuum pump, or a stream sweeping technique [6–8]. It is widely used in liquid separation, especially the separation of the azeotropic solution and close-boiling mixture. In the past decades, great achievements in PV have been made both in academic and industrial fields [6,9,10]. The first breakthrough in PV application for ethanol dehydration was achieved by the GFT Corporation in the 1980s and the first industrial-scale PV plant was put into operation in France in 1988 [6]. According to incomplete statistics [11,12], more than 60 PV units have been operating around the world till this date. As for the PV desulfurization of gasoline, a number of advantages, such as low octane number loss, high efficiency, low capital, and operation cost [13] are offered. PV desulfurization serves as the most promising technique for gasoline desulfurization.

A polymeric or an inorganic membrane is used in PV desulfurization as the separation barrier and it plays the most important role. A great deal of work has been done in exploring for polymeric membrane with a higher PV performance. A number of polymers such as polydimethylsiloxane (PDMS) [14–16], PDMS/ceramic composite membrane [17], PDMS filled with zeolite [18], hydroxyl-terminated poly(butadiene acrylonitrile) [19], polyethersulfone [20], polyimide [21], and so on have been investigated for potential application in gasoline desulfurization. Among these, polyethylene glycol (PEG), exhibits great sulfur removal capacity. As regards its easier swelling and unstable PV performance, the cross-linking modification method is applied and better PV performance is thus obtained [22]. Later on, the PEG PV membrane started to become widely investigated in PV desulfurization. The effect of sulfur component [23], feed temperature, operating conditions [24], amount of cross-linking agent, cross-linking time, and temperature for cross-linking [25] on the desulfurization performance and sorption behavior of PEG PV membrane is investigated. Simulation and design for the scale-up of PV desulfurization based on PEG PV membrane is also proposed [13]. However, the impact of solvent used in the membrane preparation has never been studied. Meanwhile, as the most challengeable component to be separated in gasoline desulfurization, thioether is rarely investigated. In this work, four types of solvents were selected to prepare the cross-linked PEG/polyvinylidene fluoride (PVDF) composite membranes (PPCMs) using PVDF as the porous supporting layer. High sulfur enrichment factor and total PV flux for the removal of thioether from ethyl thioether/heptane mixtures were obtained. According to the

characterization data and the following analysis, suggestions on the mass transfer mechanism of the sulfur containing component were made.

2. Experimental

2.1. Materials

PEG ($M_w \sim 100,000$) was obtained from Acros Organics (Geel, Belgium). PVDF was purchased from Solvay Chemicals, Belgium. Solvents for the preparation of the PPCMs were triethyl phosphate, tetrahydrofuran (THF), acetone, and ethanol that were obtained from Fucheng Chemicals (Tianjin, China), Beijing Modern Eastern Fine chemicals (Beijing, China), and Sinopharm Chemical Reagent Co., Ltd. (Beijing, China), respectively. Maleic anhydride used for the cross-linking of the prepared composite membranes was obtained from Sinopharm Chemical Reagent Co. Ltd. and trimethylamine solution (33 wt.%) was used as a catalyst in the cross-linking process. Heptane and ethyl thioether which was mixed and used as a feed mixture in the PV experiments, were purchased from Beijing Chemical Company (China). Deionized water was used throughout the entire research work. All the reagents were of analytical reagent grade and were used as-received.

2.2. Membrane preparation

2.2.1. Preparation of the PVDF supporting layer

PVDF was dissolved in triethyl phosphate to form a 15 wt.% homogeneous solution after being dried at 80°C for about 24 h to remove the trace amount of water absorbed during transport and storage. The solution was kept at 85°C for about 24 h under vigorous stirring to get the PVDF fully dissolved. Then it was filtered to remove the insoluble impurities. The filtered solution was kept under vacuum at room temperature for at least 4 h to get rid of the air bubbles formed during stirring. After degassing and cooling, the PVDF solution was cast onto the nonwoven fabrics, which was immediately immersed at room temperature into the water bath. Before the complete removal of solvent, the precipitated PVDF ultrafiltration membrane was washed several times with deionized water. Finally, the membrane was gathered for further use after water evaporation at room temperature.

2.2.2. Preparation of PEG separation layer

Different solvents, i.e. THF, acetone, and ethanol, were mixed with deionized water to form a solvent mixture at the weight ratio of 1:1, respectively. Three

major factors are considered during the selection of solvents, i.e. (1) the solvents can be used for the preparation of PEG membrane; (2) the solvents are miscible with water at the concentration given in this work; and (3) the solvents cannot dissolve the PVDF support. PEG mixed with 16 wt.% of maleic anhydride was dissolved in the solvent mixture to form a 15 wt.% homogeneous solution at room temperature. Before the casting of the formed mixture, 3 wt.% of the catalysts, i.e. the trimethylamine solution, was added. After filtration and degassing, the solution was cast onto the PVDF supporting layer with a stainless steel knife. To completely evaporate the solvent, the cast membrane was kept at room temperature for at least 10 h. Finally, the composite membranes were cross-linked at 80 °C for 5 h. After cooling at room temperature, the prepared PV membranes were collected for further characterization. The obtained membranes are designated as T-PEG, A-PEG, E-PEG, respectively, as per the respective organic solvent such as THF, acetone, and ethanol used in the membrane preparation process. In order to investigate the effect of solvent on the PV properties of PPCMs, a control labeled as W-PEG was established by using 100 wt.% of deionized water as the membrane preparation solvent. The prepared PPCMs were kept in a clean and dry circumstance before use.

2.3. Membrane characterization

2.3.1. Fourier transform infrared spectroscopy (FTIR-ATR)

Fourier transformed infrared spectra in combination with attenuated total reflectance technique (FTIR-ATR) were recorded using a Nicolet IR 560 spectrometer with a horizontal ATR accessory equipped with a ZnSe crystal. The spectra of the samples were recorded in the range of 400–4,000 cm^{-1} with a resolution of 4 cm^{-1} . Each spectrum of the membranes was collected 32 times to ensure accuracy. To get rid of the influence of the trace amount of water absorbed in storage, the samples were dried at about 30 °C using an infrared light source before testing.

2.3.2. Scanning electron microscopy

PEG/PVDF composite membranes were fractured in liquid nitrogen, coated with Au/Pd in vacuum. The cross-section morphologies of the membranes were investigated by scanning electron microscopy (SEM) at 15 kV with a Quanta 200 FEG scanning microscope (FEI Company, The Netherlands).

2.3.3. Wide-angle X-ray diffraction

The crystallinity of each of the membranes was characterized by the wide-angle X-ray diffraction (WAXD) technique at room temperature using a Bruker's advanced wide-angle X-ray diffractometer (Bruker, Germany). The X-ray source was nickel-filtered $\text{Cu-K}\alpha$ radiation (40 kV, 40 mA). The dried membranes were mounted on a sample holder and scanned in the reflection mode at an angle 2θ over a range of 3°–70° at a speed of 4°/min.

2.3.4. X-ray photoelectron spectroscopy (XPS) analysis

Surface chemical composition of PEG/PVDF composite membranes was analyzed by PHI Quantera SXM XPS instrument (ULVAC-PHI, USA) using an Al $\text{K}\alpha$ as the radiation source. The take-off angle of the photoelectron was set at 45°. Survey spectra were collected over the range of 0–1,200 eV with a resolution of 0.5 eV. High-resolution spectra of C1s and O1s peak were also collected to analyze the structural rearrangement of the membrane surface.

2.4. PV experiments

PV experiments were carried out using a self-designed apparatus, as shown in Fig. 1. The feed tank was filled with a mixture of heptane and ethyl thioether, which was continuously circulated in the upstream of the membrane by a pump. PV membrane was positioned in a stainless steel membrane cell. The effective area of the membrane in contact with the feed solution was about 21.67 cm^2 . When the system was online, the feed mixture was pumped from the tank and circulated around the upstream of the membrane. As regards the most acceptable solution-diffusion

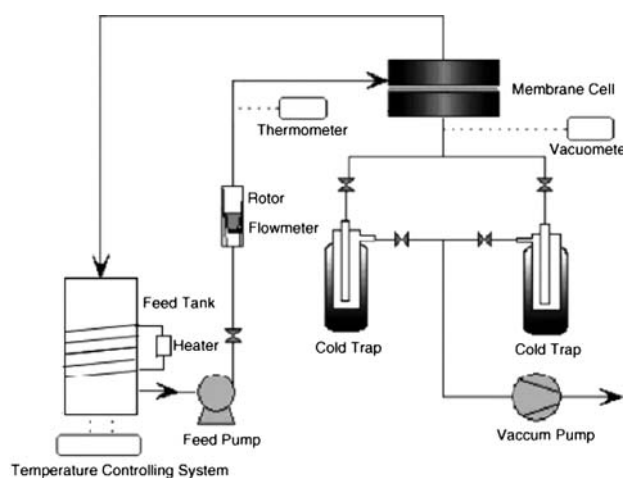


Fig. 1. Schematic representation of the PV apparatus as presented in [25].

model, three major steps occurred in a PV process: (1) sorption of the permeate to the membrane; (2) diffusion of the permeate in the membrane; and (3) evaporation of the permeate at the downstream side of the membrane. When a polymeric membrane came into contact with the liquid mixture, one component in the feed can be preferentially enriched due to its higher affinity.

In this study, the upside of the membrane was maintained at atmospheric pressure and the downside of the membrane was maintained at a pressure of less than 300 Pa using a vacuum pump. After a steady flow was obtained, the permeated mixture was collected. Then, the total sulfur content was analyzed by a Micro-Coulometric Analysis Instrument (Jiangsu, China) with an inherent difference of less than 5%. Each concentration was based on more than two injections and the PV results can be reproduced. The separation performance of the PPCMs was assessed by two major parameters: the sulfur enrichment factor and the total flux. The total PV flux J was determined by dividing the weight of the permeate with the time and the effective membrane area, as in Eq. (1).

$$J = \frac{\Delta m}{S \cdot \Delta t} \quad (1)$$

where Δm is the total amount of the permeated mixture during the experimental time interval Δt and S is the effective membrane area in contact with the feed solution. The sulfur enrichment factor, E , was defined by the following equation.

$$E = \frac{C_P}{C_F} \quad (2)$$

where C_P and C_F are the total sulfur contents of the permeate samples and the feed mixture, respectively.

3. Results and discussion

To fully understand the effect of solvent used in the membrane preparation process on the PV performance of the membrane, four types of membranes were prepared, designated as E-PEG, T-PEG, A-PEG, and W-PEG, respectively. The prepared membranes were characterized considering the relationship between PV performance and microstructure. The results will be presented and discussed in detail in the following sections.

3.1. FTIR

The ATR technique enables the identification of specific groups located within about 100 nm from the surface layer and it is widely used to characterize the

surface properties of a specific material. The molecular composition of a PEG polymer is pretty simple and it is very convenient to monitor the surface structure of the PEG membrane by the FTIR-ATR technique.

In this study, the FTIR spectroscopy is used to characterize and rudely quantify groups of the PPCMs. The FTIR spectra of typical PEG membrane are carefully examined and presented in the literature [24,25]. Nevertheless, the full-range examination of the PEG composite membrane does not assume so much significance in this study since the most important groups in the PEG molecules are $-\text{CH}_2-$, C–O. The vibration absorption of the C–O group gives out too many signals and it is easily influenced by the circumstance. Therefore, the absorbance of the $-\text{CH}_2-$ group becomes the most important signal to illustrate the structural rearrangement of the PPCMs prepared in different solvents. Fig. 2 shows the FTIR spectra of the E-PEG, T-PEG, A-PEG, and W-PEG membranes. The peak around $2,900\text{ cm}^{-1}$ indicates the existence and the quantity of the $-\text{CH}_2-$ group as labeled in the red circle (Fig. 2). Comparing the FTIR spectra of the four different PPCMs, no difference in functional groups is found, despite a slight difference in intensity. As an indicator, the difference in intensity of the $-\text{CH}_2-$ implies group rearrangement on the membrane surface. The difference in composition of mixed organic solvents means different solvent evaporating rate in membrane preparation. Thus, the four PPCMs investigated in this paper exhibit different time for surface rearrangements in the formation of composite membrane, which in turn influences the intensity of the $-\text{CH}_2-$ group reflected in the FTIR spectra. As can be clearly seen in Fig. 2, the T-PEG presents the strongest intensity, which is probably due to a longer rearranging time during the preparation process. However, since the FTIR spectra of the membranes might be influenced by so many causes, the difference in absorbance intensity is just considered to be an important indicator of the membrane surface rearrangement. It cannot be assured till accurate characterization is made.

3.2. Scanning electron microscopy

SEM micrographs of the cross-section morphology of the E-PEG, T-PEG, A-PEG, and W-PEG are presented in Fig. 3(a)–(d) respectively. The visualized thickness of the PEG separation layer is labeled in Fig. 3 and summarized in Table 1. All these four composite membranes show a relatively thin separation layer with a thickness over the range of 14–20 μm and E-PEG is the thinnest among all the four types of PPCMs having a thickness of about 14 μm , which

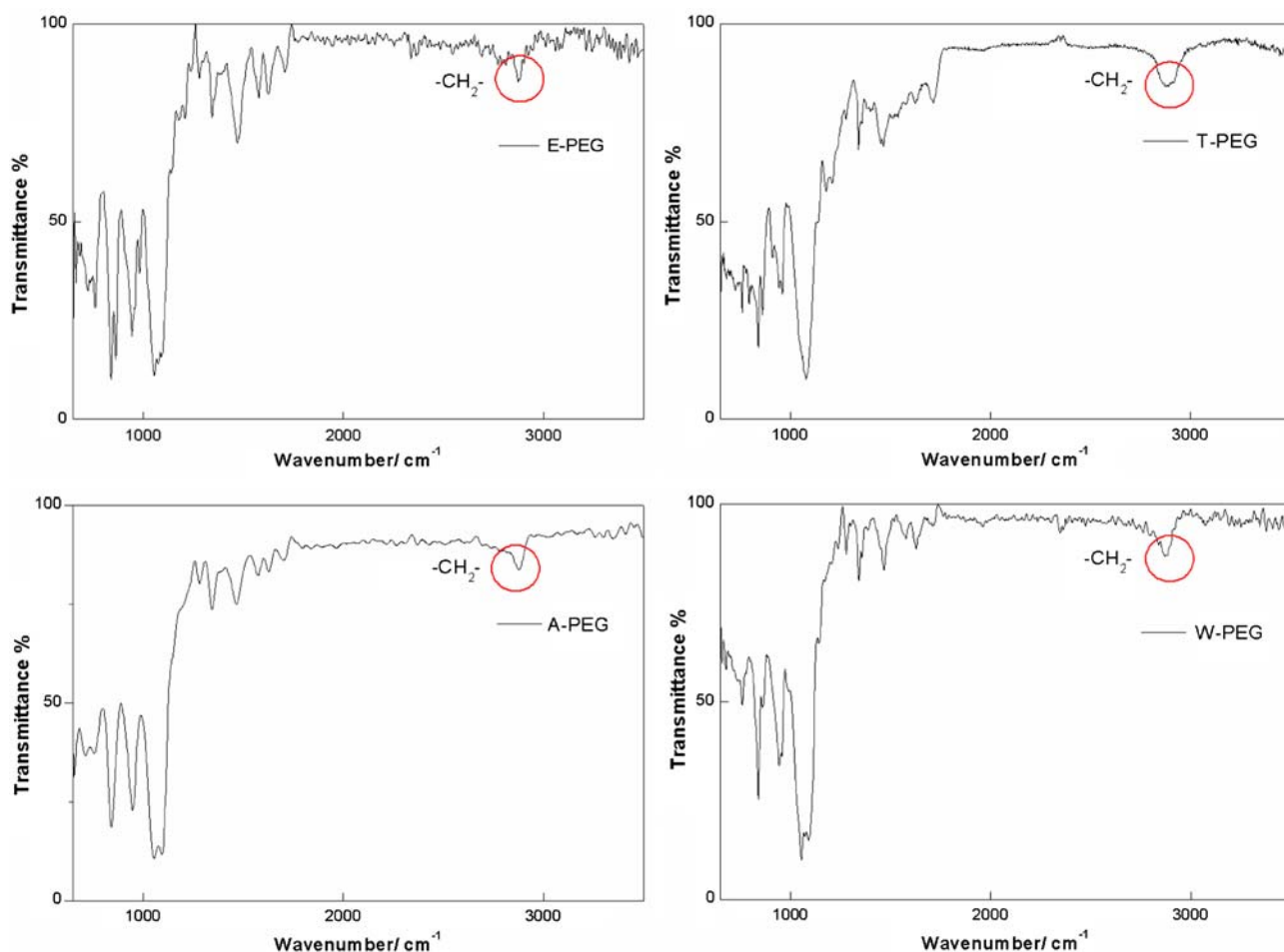


Fig. 2. FTIR spectra of the E-PEG, T-PEG, A-PEG, W-PEG composite membranes.

means a potential high separation flux than the others. The PPCMs are composed of two different layers, the separation layer and the porous supporting layer as can be observed in Fig. 3. It can also be clearly seen in these photographs that the PEG separation layer is closely cemented on the porous PVDF supporting layer with a slight intrusion of the PEG supporting layer into the porous supporting layer. It is believed that the intrusion of the membrane casting solution into the porous supporting layer will to some extent decrease the PV flux of the PPCMs in PV experiment [26].

3.3. X photoelectron spectroscopy

XPS was employed to investigate the surface oxygen aggregation of PPCMs and to help establish the relevance with their PV performance. Fig. 4 presents a full profile of 1s energy level on the surface of PPCMs. Peaks at about 280 and 520 eV indicate the existence of carbon and oxygen, respectively.

Comparing the obtained four XPS spectra of PPCMs, E-PEG, T-PEG, A-PEG, and W-PEG show a large difference in intensity, which means great difference in the surface atom composition. The oxygen concentration of PPCMs is thus calculated and is tabulated in Table 2. The results reveal that the surface oxygen composition increases in the following order: A-PEG < T-PEG < E-PEG < W-PEG.

The change in surface oxygen content indicates group rearrangements of the PPCMs. According to the analyzing of the structure of PEG, Fig. 5 illustrates the possible group rearrangement of the PEG main chains. Fig. 5(c) is not very much possible in a PEG membrane since it possesses the highest surface energy in air. In the case of PEG solution, the polymer chain movement is not hindered and thus the structure in Fig. 5(a) dominates the conformation. However, as the solvent is evaporating, the high surface energy between PPCMs and the circumstance makes the structure in Fig. 5(b) the favorite conformation. It is commonly accepted that the rearrangement of a polymer chain is relatively

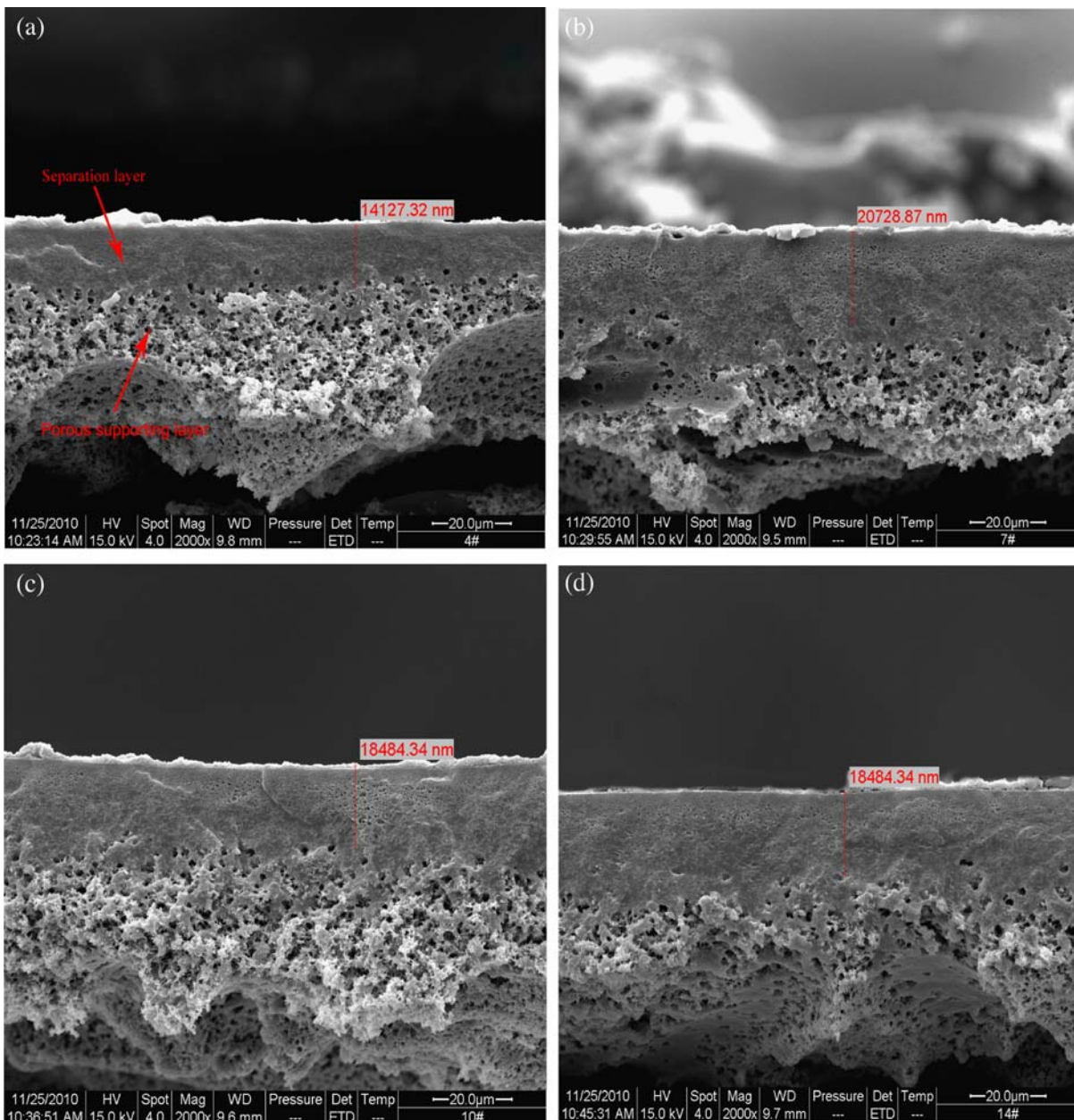


Fig. 3. SEM micrographs of cross-section morphology of the PPCMs: (a) E-PEG, (b) T-PEG, (c) A-PEG, and (d) W-PEG.

Table 1
Visualized thickness of the PPCMs measured from SEM micrographs

Membrane	Micrographs	Visualized thickness/ μm
E-PEG	Fig. 3(a)	14.13
T-PEG	Fig. 3(b)	20.73
A-PEG	Fig. 3(c)	18.48
W-PEG	Fig. 3(d)	18.48

slow. As a result, different evaporating rate means different quantity of transformation in the structure as

shown in Fig. 5(a)–(c), resulting in the different surface oxygen content. As it is being analyzed, the surface rearrangements of PPCMs do exist. Thus, different PV performance can be clearly foreseen.

3.4. WAXD

Different from the inorganic compound, the crystal of organic polymers is not perfect. Amorphous region coexists with crystalline region. Thus, crystallinity is introduced to assess the polymer crystal and WAXD

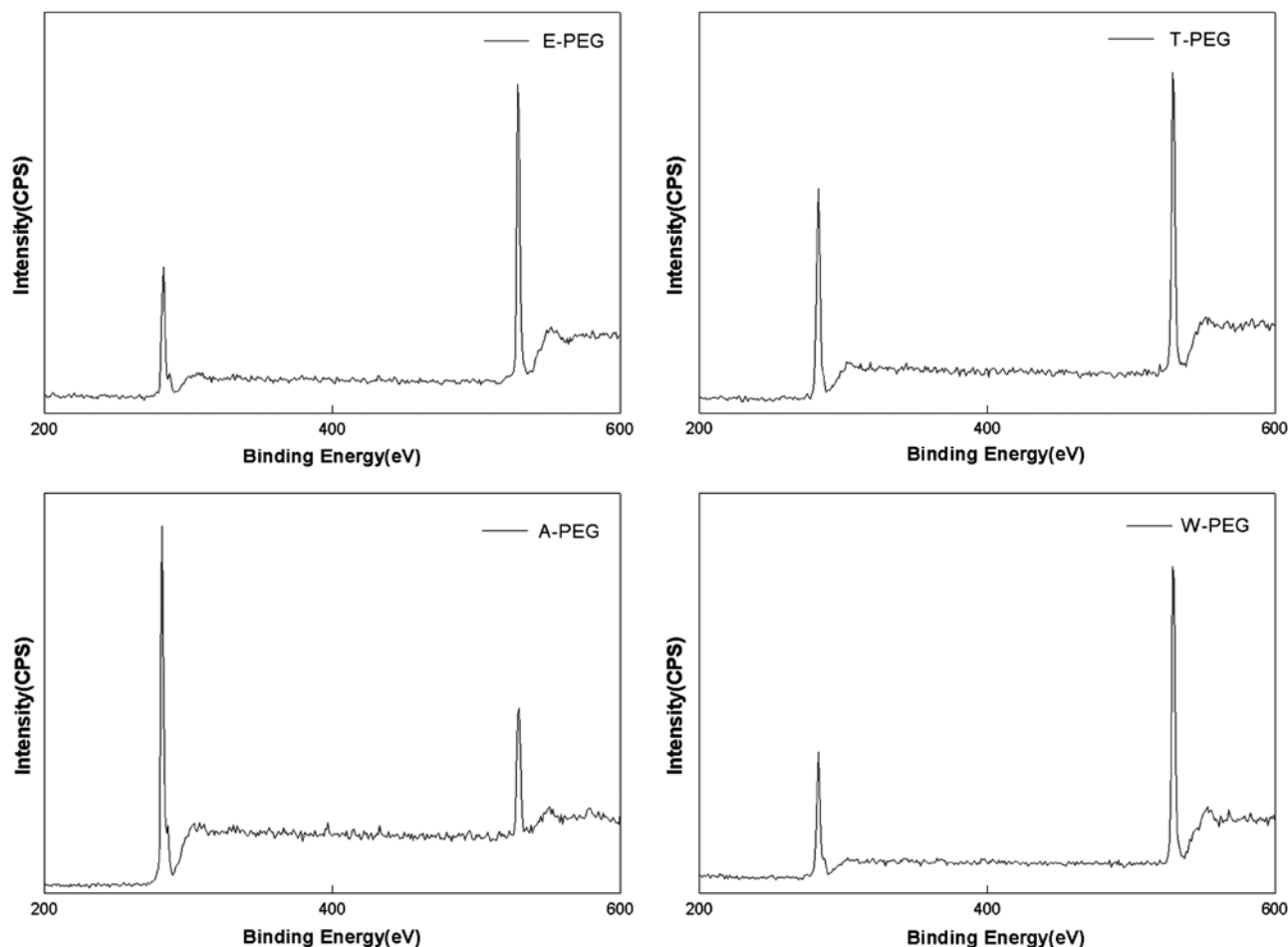


Fig. 4. XPS spectra of the E-PEG, T-PEG, A-PEG, and W-PEG composite membranes.

Table 2
Calculated crystallinity and surface oxygen content of the PEG/PVDF membrane

PEG/PVDF membrane	Crystallinity (%)	Surface oxygen concentration (%)
E-PEG	48.67	43.19
T-PEG	62.01	35.06
A-PEG	74.87	14.98
W-PEG	73.30	47.16

becomes the most commonly used method to get a full image of the polymer crystal. The WAXD studies not only indicate the nature of the compounds but also enable the identification of the structural parameters of the polymer crystal.

To establish the relationship between the microstructure of the membrane and the PV performance, WAXD is employed. The obtained profiles are

presented in Fig. 6. It is observed that the crystalline diffraction peaks of the PPCMs are at around 19° and 23° , and they show good accordance with the literature [27]. The diffraction patterns of the E-PEG, T-PEG, A-PEG, and W-PEG are almost the same, despite the difference in intensity. The wide-angle covered region around the baseline implies the existence of the amorphous region and crystallinity can thus be calculated using the following equation

$$\omega_c = \frac{A_c}{A_c + A_a} \quad (3)$$

where ω_c is the crystallinity of the polymer, A_c and A_a stand for the area of the crystalline region and amorphous region, respectively.

According to Eq. (3), the peak fitting process is employed to calculate the crystallinity of the PPCMs. The result is presented in Table 2. The crystallinity of the PEG/PV membrane increases in the following order: E-PEG < T-PEG < W-PEG < A-PEG. The difference in

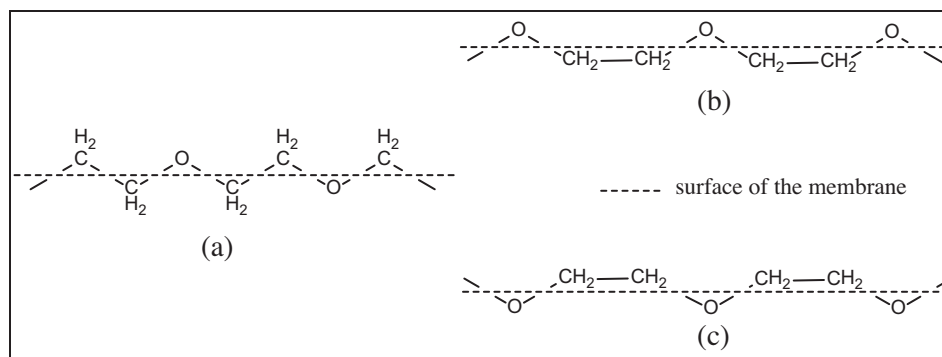


Fig. 5. Possible surface rearrangements of PEG.

intensity reflected in the WAXD spectra is due to the difference in evaporating rate of the solvent mixtures. As commonly accepted, the formation of polymer crystal is due to the regularly arranged polymer main chains and the rearrangement of polymer main chains is a time-dependent process. Thus, a rapid evaporation of solvents makes it relatively impossible for the polymer main chains to rearrange, which consequently gives out more amorphous region in the polymer crystal. It can be concluded from Table 2 that the ethanol–water mixture used for the preparation of E-PEG possesses the most rapid evaporating rate.

3.5. PV performance

PV experiments were conducted at four different temperatures, i.e. 80, 75, 70, and 65°C, with a feed sulfur content of around 300×10^{-6} kg/L. The flux and the sulfur enrichment factor of the four different PPCMs at different temperatures are presented in Figs. 7 and 8, respectively. The results show that the prepared composite membranes have great PV performance for desulfurization of model gasoline. Details will be discussed in the following sections.

3.5.1. The effect of temperature

The temperature shows a great impact on the PV performance of the PPCMs. It is observed in Figs. 7 and 8 that the PV flux increases, while the sulfur enrichment factor decreases with an increase in the temperature. It is commonly accepted that the movement of the polymer chain must be activated. Thus, as the temperature increased, more energy is input into the PEG matrix and the movement of the PEG main chain becomes much easier. An easier main chain movement means less mass transport resistance to the heptane and ethyl thioether transportation. Consequently, a higher separation flux and a lower sulfur enrichment factor are obtained. It is also observed,

that the trend is correct in any of the four PPCMs. Nevertheless, different changing rates are also observed which means different mass transfer activation energy [28].

3.5.2. The effect of solvent

The idea of changing organic solvent in the membrane preparation process originates from a US patent [29] in which methanol was used as mass transfer facilitation in desulfurization and a pretty high separation factor was obtained. In order to investigate the effect of solvent on PV performance, four types of solvents are thus applied in the preparation of PPCMs in this work. The obtained PV experiment results are presented in Figs. 7 and 8.

It is observed that in the temperature range of 65–75°C, the sulfur enrichment factor of the four PPCMs decreases in the following order: E-PEG > T-PEG > W-PEG > A-PEG. E-PEG shows the highest separation factor of about 5.3 for the removal of sulfur from the feed mixture and A-PEG performs the worst with a sulfur enrichment factor of no more than 3.5.

In the study of the effect of solvent on separation flux of the PPCMs, T-PEG, A-PEG, and W-PEG exhibit a similar separation flux of about $0.1 \text{ kg}/(\text{m}^2\text{h})$ with the same order of magnitude. Low separation flux of PPCMs is attributed to the thicker separation layer and the intrusion of casting solution into the porous supporting layer, which can be clearly seen in the SEM micrographs (Fig. 3). However, the E-PEG presents a pretty high separation flux, than the rest because of its smallest thickness of about $14 \mu\text{m}$. Considering the requirements of industrial application, the E-PEG membrane shows both the highest sulfur enrichment factor and the separation flux which means great application potential. Unfortunately, the exact mechanism on how the solvents influence the PV performance cannot be fully understood till a full image of the microstructure of the PPCMs is depicted.

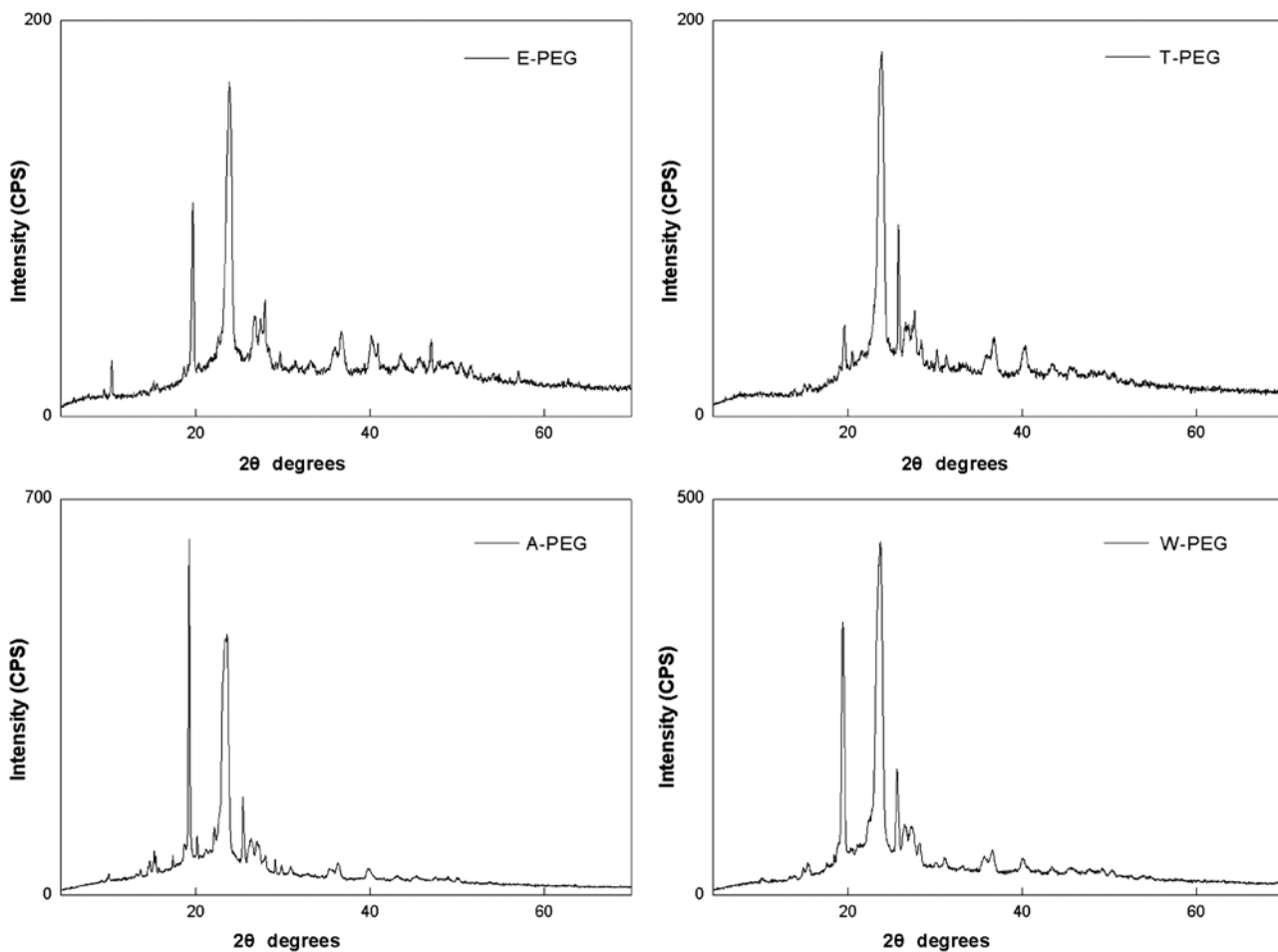


Fig. 6. XRD patterns of the E-PEG, T-PEG, A-PEG, and W-PEG composite membranes.

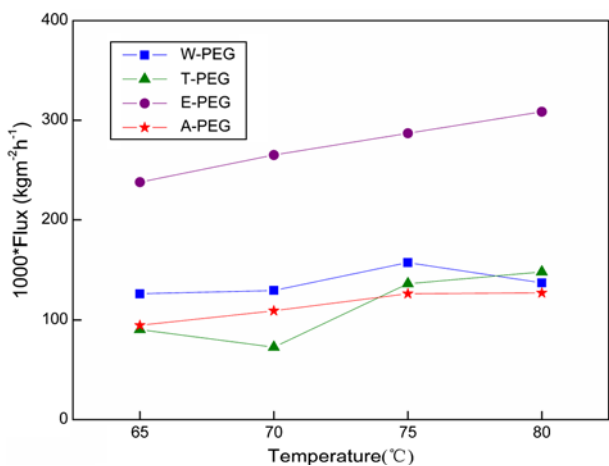


Fig. 7. Effect of temperature and solvent on the PV flux of the PPCMs.

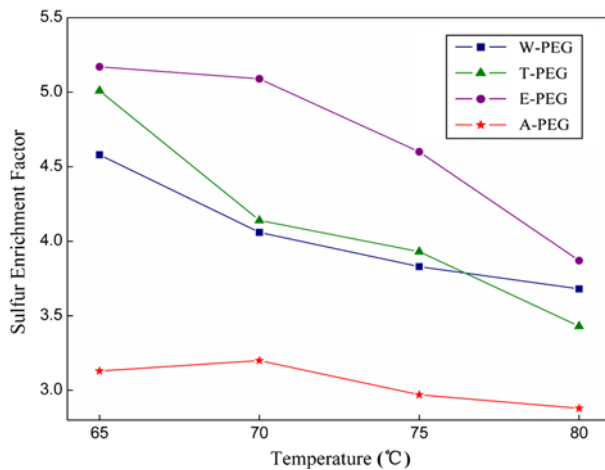


Fig. 8. Effect of temperature and solvent on the sulfur enrichment factor of the PPCMs.

Thus, it was an urgent work to establish the relationship between the microstructure of PPCMs and its PV performance.

3.6. The microstructural relationship with the PV performance

The change in microstructure of the PPCMs is caused by the change of solvent composition. As can be concluded from the discussions above, different solvent composition means different evaporating rate of solvents resulting in a great difference in polymer main rearrangements and surface group rearrangements. A low evaporating rate means sufficient time for the formation of crystalline region and the transformation of surface groups reflected by a high crystallinity and high surface oxygen content in this work. Hence, it is very pivotal to establish the correlation of crystallinity and surface oxygen aggregation with the PV performance of PPCMs in order to investigate the influence of solvent on the PV performance of PPCMs. The PV performance of PPCMs is investigated at 75°C due to the concerns of both feed mixture stableness and the accuracy of flux.

3.6.1. Membrane crystallinity

It is observed from the WAXD spectra of the E-PEG, T-PEG, A-PEG, and W-PEG composite membranes that the use of different solvents produces membranes with different crystallinity. Fig. 9 correlates the crystallinity of PPCMs with its PV performance. It can be clearly observed that both sulfur enrichment factor and PV flux decreases with an increase in crystallinity. It is believed that the crystalline region of the PPCMs exhibits stiff resistance to the mass transfer of heptane and ethyl thioether. As the crystallinity increases, the resistance for cross-linking and mass transportation increases resulting in a decrease in PV flux. A decrease in sulfur enrichment factor is attributed to the decrease of effective separation region. It is suggested that higher cross-linking density allows higher sulfur enrichment factor [25]. Thus, the decrease in cross-linking will absolutely decrease the effective separation area that subsequently decreases the sulfur enrichment factor of the PPCMs.

3.6.2. Oxygen aggregation

The surface oxygen content of PPCMs is obtained using the XPS technique and the obtained surface oxygen content is correlated to the PV performance of PPCMs (Fig. 10). It is observed that an increase in surface oxygen content leads to an increase in both

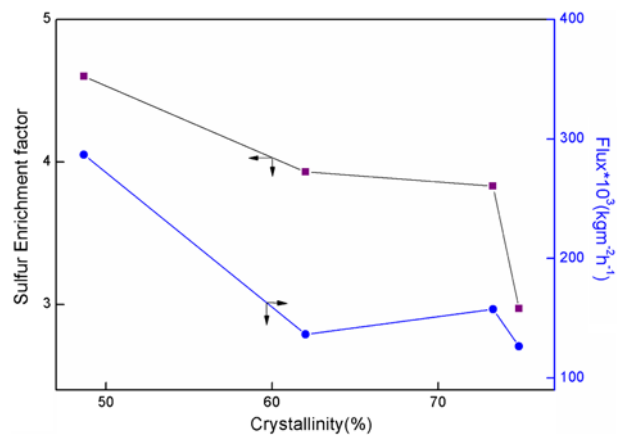


Fig. 9. Effect of crystallinity on the PV performance of PPCMs at 75°C.

separation flux and sulfur enrichment factor over the surface oxygen content range of 14.98–43.19%. It can be explained by the similarity of sulfur to oxygen. Consequently, a higher surface oxygen content results in higher sorption of the sulfur-containing compound at the membrane surface which might cause an improvement in the PPCMs. However, a sharp decrease is observed as the surface oxygen content exceeded 45%. A sudden decrease of both sulfur enrichment factor and separation flux is attributed to a pretty high crystallinity of 73.30% for the W-PEG composite membrane. As regards the discussion in Section 3.5.1, it can be suggested that high surface oxygen content and low crystallinity contribute significantly to the improvement of PPCMs. Subsequently, we can conclude here that E-PEG performed the best and A-PEG the worst in the PV experiments according to Table 2, which is in accordance with PV performance of the PPCMs as presented in Figs. 7 and 8.

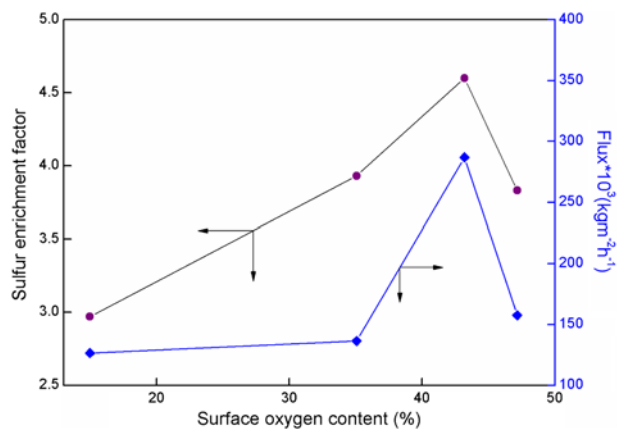


Fig. 10. Impact of surface oxygen content on the PV performance of PPCMs at 75°C.

4. Conclusion

PPCMs were successfully prepared using different solvent mixtures and the obtained PPCMs showed good sulfur removal ability. At the same time, solvents have a huge impact on the PV performance of the PPCMs. E-PEG exhibits the best PV performance in this work. The high separation performance of the E-PEG composite membrane is due to the synergistic effect of membrane crystallinity and surface oxygen content. It can be concluded that high surface oxygen content leads to high sorption of ethyl thioether at the surface resulting in a better PV performance. The impact of membrane crystallinity is based on the resistance of the crystalline region to cross-linking and mass transportation. An increase in crystallinity results in an increase in cross-linking and mass transportation resistance leading to an obvious decrease in PV performance of the PPCMs. The above conclusion implies that the influence of membrane crystallinity and surface oxygen content should be included in the investigation of other polymeric membranes.

Acknowledgments

The authors greatly appreciate the financial support of the Major State Basic Research Program of China (2012AA03A607), National Natural Science Foundation of China (20736003, 21176135).

References

- [1] T.G. Kaufmann, A. Kaldor, G.F. Stuntz, M.C. Kerby, L.L. Ansell, Catalysis science and technology for cleaner transportation fuels, *Catal. Today* 62 (2000) 77–90.
- [2] C. Song, X. Ma, New design approaches to ultra-clean diesel fuels by deep desulfurization and deep dearomatization, *Appl. Catal., B* 41 (2003) 207–238.
- [3] I.V. Babich, J.A. Moulijn, Science and technology of novel processes for deep desulfurization of oil refinery streams: A review, *Fuel* 82 (2003) 607–631.
- [4] M. Muzic, K. Sertic-Bionda, Z. Gomzi, S. Podolski, S. Telen, Study of diesel fuel desulfurization by adsorption, *Chem. Eng. Res. Des.* 88 (2010) 487–495.
- [5] A. Seeberger, A. Jess, Desulfurization of diesel oil by selective oxidation and extraction of sulfur compounds by ionic liquids—a contribution to a competitive process design, *Green Chem.* 12 (2010) 602–608.
- [6] P. Shao, R.Y.M. Huang, Polymeric membrane pervaporation, *J. Membr. Sci.* 287 (2007) 162–179.
- [7] C. Vallières, E. Favre, Vacuum versus sweeping gas operation for binary mixtures separation by dense membrane processes, *J. Membr. Sci.* 244 (2004) 17–23.
- [8] A. Noworyta, M. Kubasiewicz-Ponitka, A. Koziol, Mass and heat transport resistance in pervaporation process, *Desalin. Water Treat.* 26 (2011) 226–235.
- [9] A. Jonquière, R. Clément, P. Lochon, J. Néel, M. Dresch, B. Chrétien, Industrial state-of-the-art of pervaporation and vapour permeation in the western countries, *J. Membr. Sci.* 206 (2002) 87–117.
- [10] D. Jeong, J. Oh, I. Yum, Y. Lee, Removal of VOCs from their aqueous solution by pervaporation with PDMS-zeolite composite membrane, *Desalin. Water Treat.* 17 (2010) 242–247.
- [11] L.M. Vane, A review of pervaporation for product recovery from biomass fermentation processes, *J. Chem. Technol. Biotechnol.* 80 (2005) 603–629.
- [12] D.J. Benedict, S.J. Parulekar, S.-P. Tsai, Pervaporation-assisted esterification of lactic and succinic acids with downstream ester recovery, *J. Membr. Sci.* 281 (2006) 435–445.
- [13] L. Lin, Y. Kong, J. Yang, D. Shi, K. Xie, Y. Zhang, Scale-up of pervaporation for gasoline desulfurization: Part 1. Simulation and design, *J. Membr. Sci.* 298 (2007) 1–13.
- [14] J. Chen, J. Li, R. Qi, H. Ye, C. Chen, Pervaporation performance of crosslinked polydimethylsiloxane membranes for deep desulfurization of FCC gasoline: I. Effect of different sulfur species, *J. Membr. Sci.* 322 (2008) 113–121.
- [15] J. Chen, J. Li, R. Qi, H. Ye, C. Chen, Pervaporation separation of thiophene–heptane mixtures with polydimethylsiloxane (PDMS) Membrane for Desulfurization, *Appl. Biochem. Biotechnol.* 160 (2010) 486–497.
- [16] C. Zhao, J. Li, J. Chen, R. Qi, Z. Luan, Separation of sulfur/gasoline mixture with polydimethylsiloxane/polyetherimide composite membranes by pervaporation, *Chin. J. Chem. Eng.* 17 (2009) 707–710.
- [17] R. Xu, G. Liu, X. Dong, Jin, Wanqin, Pervaporation separation of n-octane/thiophene mixtures using polydimethylsiloxane/ceramic composite membranes, *Desalination* 258 (2010) 106–111.
- [18] R. Qi, Y. Wang, J. Chen, J. Li, S. Zhu, Removing thiophenes from n-octane using PDMS-AgY zeolite mixed matrix membranes, *J. Membr. Sci.* 295 (2007) 114–120.
- [19] J. Chen, J. Li, X. Han, X. Zhan, C. Chen, Liquefied petroleum gas desulfurization by HTBN/PAN composite membrane, *J. Appl. Polym. Sci.* 117 (2010) 2472–2479.
- [20] B. Li, W. Zhao, Y. Su, Z. Jiang, X. Dong, W. Liu, Enhanced desulfurization performance and swelling resistance of asymmetric hydrophilic pervaporation membrane prepared through surface segregation technique, *J. Membr. Sci.* 326 (2009) 556–563.
- [21] I. Bettermann, C. Staudt, Permeation of binuclear, sulphur containing aromatic compounds, *Desalination* 250 (2010) 1144–1146.
- [22] L. Lin, Y. Kong, G. Wang, H. Qu, J. Yang, D. Shi, Selection and crosslinking modification of membrane material for FCC gasoline desulfurization, *J. Membr. Sci.* 285 (2006) 144–151.
- [23] Y. Kong, L. Lin, J. Yang, D. Shi, H. Qu, K. Xie, L. Li, FCC gasoline desulfurization by pervaporation: Effects of gasoline components, *J. Membr. Sci.* 293 (2007) 36–43.
- [24] L. Lin, Y. Kong, K. Xie, F. Lu, R. Liu, L. Guo, S. Shao, J. Yang, D. Shi, Y. Zhang, Polyethylene glycol/polyurethane blend membranes for gasoline desulfurization by pervaporation technique, *Sep. Purif. Technol.* 61 (2008) 293–300.
- [25] J. Chen, J. Li, J. Chen, Y. Lin, X. Wang, Pervaporation separation of ethyl thioether/heptane mixtures by polyethylene glycol membranes, *Sep. Purif. Technol.* 66 (2009) 606–612.
- [26] T. Fei, C. Jian, L. Jiding, W. Lei, Z. Xia, Pervaporation performance of HTBN/PAN composite membrane for separating n-heptane/diethyl sulfide/n-butanethiol mixtures, *Membr. Sci. Technol.* 31 (2011) 56–61, in Chinese.
- [27] D.O. Corrigan, A.M. Healy, O.I. Corrigan, The effect of spray drying solutions of polyethylene glycol (PEG) and lactose/PEG on their physicochemical properties, *Int. J. Pharm.* 235 (2002) 193–205.
- [28] L. Lin, G. Wang, H. Qu, J. Yang, Y. Wang, D. Shi, Y. Kong, Pervaporation performance of crosslinked polyethylene glycol membranes for deep desulfurization of FCC gasoline, *J. Membr. Sci.* 280 (2006) 651–658.
- [29] R.J. Saxton, B.S. Minhas, Ionic membranes for organic sulfur separation from liquid hydrocarbon solution, WO 02/053682, 2002.